molecular pharmaceutics

ARTICLE

pubs.acs.org/molecularpharmaceutics

Gene-Modified Adult Stem Cells Regenerate Vertebral Bone Defect in a Rat Model

Dmitriy Sheyn,[†,‡] Ilan Kallai,[‡,§] Wafa Tawackoli,[†,‡] Doron Cohn Yakubovich,[§] Anthony Oh,[†] Susan Su,[†] Xiaoyu Da,[†] Amir Lavi,[§] Nadav Kimelman-Bleich,[§] Yoram Zilberman,[§] Ning Li,[∥] Hyun Bae,[¶] Zulma Gazit,[†,§] Gadi Pelled,[†,§] and Dan Gazit*[,†,§]

[†]Department of Surgery and Cedars-Sinai Regenerative Medicine Institute (CS-RMI), Cedars-Sinai Medical Center, Los Angeles, California, USA

[§]Skeletal Biotech Laboratory, The Hebrew University—Hadassah Faculty of Dental Medicine, Ein Kerem, Jerusalem, Israel

[∥]Biostatistics and Bioinformatics Division Samuel Oschin Comprehensive Cancer Institute, Cedars-Sinai Medical Center, Los Angeles, CA, USA

[¶]Department of Surgery, Spine Center, Cedars Sinai Medical Center, Los Angeles, CA, USA

ABSTRACT: Vertebral compression fractures (VCFs), the most common fragility fractures, account for approximately 700,000 injuries per year. Since open surgery involves morbidity and implant failure in the osteoporotic patient population, a new minimally invasive biological solution to vertebral bone repair is needed. Previously, we showed that adipose-derived stem cells (ASCs) overexpressing a BMP gene are capable of inducing spinal fusion in vivo. We hypothesized that a direct injection of ASCs, designed to transiently overexpress rhBMP6, into a vertebral bone void defect would accelerate bone regeneration. Porcine ASCs were isolated and labeled with lentiviral vectors that encode for the reporter gene *luciferase* (*Luc*) under constitutive (ubiquitin) or inductive (osteocalcin) promoters. The ASCs were first labeled with reporter genes and then nucleofected with an rhBMP6-encoding plasmid. Twenty-four hours later, bone void defects were created in the coccygeal vertebrae of nude rats. The ASC-BMP6 cells were suspended in fibrin gel (FG) and injected into the bone void. A control group was injected with FG alone. The regenerative process was monitored in vivo using microCT, and cell survival and differentiation were monitored using tissue specific reporter genes and bioluminescence imaging (BLI). The surgically treated vertebrae were harvested after 12 weeks and subjected to histological and immunohistochemical (against porcine vimentin) analyses. In vivo BLI detected *Luc*-expressing cells at the implantation site over a 12-week period. Beginning 2 weeks postoperatively, considerable defect repair was observed in the group treated with ASC-BMP6 cells. The rate of bone formation in the stem cell-treated group was two times faster than that in the FG-treated group, and bone volume at the end point was 2-fold compared to the control group. Twelve weeks after cell injection the bone volume within the void reached the volume measured in native vertebrae. Immunostaining against porcine vimentin indicated that the ASC-BMP6 cells contributed to new bone formation. Here we show the potential of injections of BMP-modified ASCs to repair vertebral bone defects in a rat model. Our results could pave the way to a novel approach for the biological treatment of traumatic and osteoporosis-related vertebral bone injuries.

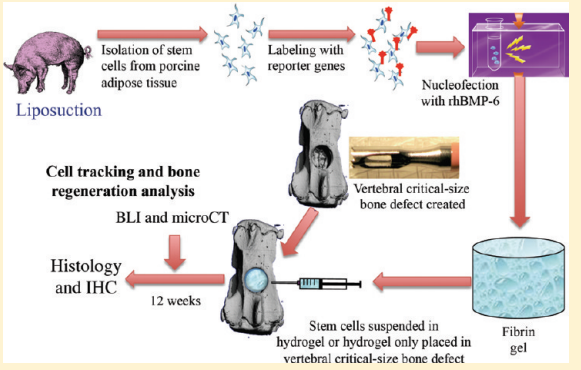

KEYWORDS: vertebral fracture, bone regeneration, gene-and-cell therapy, stem cell tracking

INTRODUCTION

The lifetime incidence of osteoporosis-related fragility in patients older than 50 years of age is approximately 1 in 2 in women and 1 in 4 in men.[1] In the year 2007, osteoporosis was estimated by the World Health Organization to affect 200 million women worldwide: approximately one-tenth of women aged 60, one-fifth of women aged 70, two-fifths of women aged 80 and two-thirds of women aged 90.[2] Vertebral compression fractures (VCFs) are the most common injuries resulting from osteoporosis. Every year an estimated 1−4 million vertebral compression fractures that cause pain and disability and diminish quality of life[3,4] come to clinical attention worldwide.[5]

In the past VCFs received limited attention from the spine care community. This oversight may have been due to the perception that VCFs are benign, self-limited problems or that treatment options are limited. However, it has become clear that VCFs are associated with significant physiologic and functional impairments, even in patients who do not seek medical care at the time of fracture.[6]

In addition to the elderly osteoporotic population most affected by VCFs, a new population of younger sufferers of VCFs

Special Issue: Emerging Trends in Gene- and Stem-Based Combination Therapy

Received: May 2, 2011
Accepted: August 11, 2011
Revised: August 2, 2011
Published: August 11, 2011

has emerged. Low-lumbar burst fractures are the predominant combat-related spine injury in the current Iraq and Afghanistan military conflicts.[7] Spine fractures have serious consequences for active soldiers and their ability to return to duty. In their retrospective review, Islinger et al. reported that 64% of soldiers who suffered from thoracolumbar spine fractures did not return to their previous duties.[8] In another study, Kornberg and colleagues found that only 28% of active-duty military personnel who sustained similar fractures were retained on active-duty rosters.[9] Spine fractures may greatly affect army aviators as well. According to the U.S. Army aeromedical standards for aviation service, all aviators with thoracolumbar fractures are initially disqualified regardless of whether their treatment entailed surgery. Belmont et al. studied the thoracolumbar fractures identified during medical assessment of 33,365 army aviators; 40% of the fractures were classified as burst fractures and 53% as compression fractures. Compression fractures are mostly found in paratroopers and helicopter pilots, whereas burst fractures are typical injuries sustained by members of special operations units.[10] A third type of fracture, caused by blast, can lead to penetrating fractures of the spine and can be the result of various explosions.

Current treatment of osteoporotic patients is focused mainly on prevention of VCFs by prescribing new medications such as alendronate and parathyroid hormone (1−34).[11,12] There are few treatment options after VCFs actually occur. Since open surgery involves morbidity and implant failure in the osteoporotic patient population, the vast majority of patients are offered nonoperative management, including medications and bracing. Unfortunately, many patients report intractable pain and the inability to return to normal activities. The limitations of nonoperative management have fostered increased interest in new, minimally invasive surgical techniques. Because fracture biomechanics are primarily determined by disruption of the trabecular microarchitecture[13] and since ongoing symptoms may be related to ineffective structural repair and motion, new nonbiological methods have been developed to regain healthful biomechanical properties in the vertebral body. These nonbiological methods include the minimally invasive procedures of vertebroplasty and balloon tamp reduction. Both procedures involve percutaneous injection of polymethylmethacrylate (PMMA) into the collapsed spinal vertebral body.[6,14] A recent study suggests that a prophylactic injection of PMMA into osteoporotic vertebrae maintains higher vertebral stiffness than a postfracture injection.[15] Moreover, according to two recent prospective studies reported in the *New England Journal of Medicine*, treatment with PMMA vertebroplasty is no more effective than sham treatment.[16,17] Thus, currently there is no efficient biological solution for the treatment of VCFs.

There have only been a couple of studies in which researchers attempted to induce vertebral bone regeneration using a biological approach. Defects were created in the lumbar vertebrae of sheep, and regeneration was induced by using autologous bone grafts[18] or OP-1 protein therapy.[19] Neither approach resulted in statistically significant bone repair compared to the untreated controls.[18,19]

Previously we showed that genetically modified adult stem cells have several advantages over protein therapy or use of autologous bone grafts in bone regeneration. Mesenchymal stem cells (MSCs) constitute a population of cells in the bone marrow and adipose tissue that can differentiate into a variety of cell types, including osteoblasts, chondrocytes, adipocytes, myocytes, and tendon- or ligament-forming cells.[20−22] Genetic modification of MSCs to overexpress a bone morphogenetic protein (BMP) gene provides therapeutic protein secretion and a supply of osteogenic cells—without the need for excessive doses of BMP proteins or harvest of bone grafts from the patient. Indeed, several studies have shown the superiority of such an approach over protein therapy alone.[23,24] Earlier we showed that adult MSCs induce rapid bone regeneration and fracture repair in vivo in several models of bone loss,[25−27] including long bones,[28] the calvaria,[29,30] and the spine.[31,32] Specifically, genetically modified porcine adipose tissue-derived stem cells (ASCs) were shown to induce bone formation and spinal fusion in a rodent model.[31,33] Thus we hypothesized that porcine ASCs that were genetically modified to overexpress rhBMP6 using a nonviral method could be used to accelerate vertebral bone defect repair in a rat model. We first established a reproducible rodent model of vertebral bone loss that could enable the use of molecular optical imaging to monitor stem cell participation in the regeneration process. Next we used primary porcine ASCs to pursue the hypothesis and regenerate the lost bone tissue. The aim of this study was to lay the foundations for a novel, clinical-practice paradigm for the treatment of vertebral fractures such as VCFs.

EXPERIMENTAL SECTION

Isolation of ASCs. The Institutional Animal Care and Use Committee of Cedars-Sinai Medical Center approved all animal studies described in this paper (IACUC #002290). The ASCs were isolated from porcine adipose tissue as previously reported.[34] Briefly, adipose tissue was harvested from subcutaneous fat pads of euthanized minipigs. The harvested tissue was cut into small pieces (less than 5 mm^3), washed three times with phosphate-buffered saline containing 1% bovine serum albumin (PBS 1% BSA [Sigma, St. Louis, MO, USA]), treated with 0.1% collagenase in PBS 1% BSA, and placed on a shaker at 37 °C for 60 min. The collagenase was inactivated by an addition of complete growth medium (Dulbecco's modified Eagle's medium [DMEM, Invitrogen, Carlsbad, CA] containing 10% fetal calf serum [Invitrogen, Carlsbad, CA]). The fraction of mononuclear cells was retrieved and plated in tissue-culture dishes at a density of 5×10^6 cells per 100 mm culture plate in an atmosphere of 5% CO_2/95% air at 37 °C. The medium was changed after 72 h and every 3 to 4 days thereafter. The ASCs were expanded in culture up to the fifth passage. In experiments where osteogenic differentiation of ASCs was required in vitro, 3 commonly used osteogenic supplements were added to the culture medium: 0.1 μM dexamethasone, 0.05 mM ascorbic acid-2-phosphate, and 10 mM β-glycerophosphate (Sigma).

Genetic Modification of ASCs. A lentiviral vector[35] that harbored the reporter genes *green fluorescent protein* (*GFP*) and firefly *luciferase* (*Luc*) under the constitutive ubiquitin promoter (hereafter referred to as LUBFG [lenti ubiquitin promoter-driven firefly luciferase and GFP]) was produced in 293HEK cells by using a standard procedure.[35,36] Plasmids encoding the vector and packaging proteins of the virus were generously provided by Dr. Joseph Wu (Stanford University, Stanford, CA, USA).[35,36] Porcine ASCs were labeled with the LUBFG lentiviral vector as previously reported.[36] Briefly, the viral vector was resuspended at a MOI of 20 and a Polybrene concentration of 6 μg/mL. Porcine ASCs were cultured until they reached 80% confluence and incubated with the lentiviral vector overnight. After the cells had had time to be infected by the lentivirus, their culture medium was replaced daily for 3 days. Fluorescence microscopy was used to verify successful infection by *GFP* expression, and the cells were assessed using flow cytometry

on day 3; *Luc* expression was verified using bioluminescence imaging (BLI) in vitro (Xenogen IVIS Spectrum, Caliper Life Sciences, Hopkinton, MA, USA).

To monitor osteogenic differentiation in vivo, a new plasmid was constructed that harbored the *Luc2* reporter gene (from pGL4, Promega, Madison, WI, USA) under the regulation of the human osteocalcin promoter (Oc-Luc2). The human osteocalcin promoter was cut out from the Oc-GFP plasmid[37] and cloned into a firefly luciferase type 2-encoding pGL4 vector (Catalog No. E6751, Promega, Madison, WI, USA). The sequence containing the osteocalcin promoter and the *Luc2* gene was then cloned into a backbone of the lentiviral vector pHRUBGF,[38] which was generously provided by Dr. Eduardo Marban (Cedars-Sinai Medical Center, Los Angeles, CA, USA). Viral particles were produced in 293HEK cells by using a standard procedure,[35,36] and wild-type porcine ASCs were infected. The infection was verified using PCR with primers against the human osteocalcin promoter (forward, GCT TCC TCT TTA GAC TCC CCT AGA G; reverse, GAC CCC TCA GCT CCA ACT CA; amplicon 86bp, as published elsewere[39]) or the *Luc* reporter gene (forward, CAG GGC TTC CAA AGC ATG TAC; reverse, CGA AAG CCG CAG ATC AAG TAG; amplicon 308bp, designed using Primer Express 3.0 software). The induced bioluminescence was tested in vitro using standard osteogenic supplements,[40−42] and BLI was performed in vitro.

After the porcine ASCs had been labeled with either the LUBFG or Oc-Luc2 reporter constructs, the cells were expended in culture and nucleofected with human rhBMP6-encoding plasmid, as previously described,[31] by using a nucleofection kit and the G22 program of the Nucleofector (Lonza, Walkersville, MD). The cells were nucleofected in 2×10^6 cells per round with 10 μg of rhBMP6-encoding plasmid. After nucleofection, the cells were seeded in culture dishes for 2 h before transplantation. On the day of surgery, the viable cells, hereafter referred to as ASC-BMP6 cells, were detached, counted, washed with PBS, and aliquoted in 10^6 cells per injection.

Surgical Procedures. Cohorts of mature athymic nude rats underwent surgical procedures to create a vertebral bone void; afterward they were randomly assigned to one of three treatment groups. The animals were anesthetized by an intraperitoneal injection of ketamine (75.0 mg/kg)/dexmedetomidine (0.25 mg/kg). The third caudal vertebra (Ca3) was identified and exposed through a left posterolateral approach. The dorsal spinal muscles were cleared away from the lateral aspects of the vertebral body, and a 1.8 mm diameter trephine drill bit was used to create a cylindrical defect (~2 mm deep) in the center of the vertebral body. The defect was injected with 10^6 pASC-LUBFG cells (n = 7) or pASC-Oc-Luc2 cells (n = 6) suspended in 10 μL of fibrin gel (FG; Tisseel kit, Baxter, Vienna, Austria). The cells were pelleted, resuspened in 5 μL of thrombin and mixed with 5 μL of fibrinogen in a tuberculin syringe prior to injection into the defect site. Following this, the skin was closed using nylon sutures. Defects in the control group were created in the same manner but were treated with an injection of FG alone (n = 5). The animals healed with unrestricted activity for 12 weeks, during which bone repair was monitored using in vivo BLI (Xenogen IVIS Spectrum system, Caliper Life Sciences, Hopkinton, MA) and micro computed tomography (vivaCT 40; Scanco Medical AG, Brüttisellen, Switzerland), hereafter referred to as microCT. After the animals had been euthanized, both treated and adjacent nontreated vertebral bodies were collected for histological examinations.

Monitoring of in Vivo Stem Cell Survival and Differentiation Using BLI. Genetically modified stem cells were monitored in vivo to assess cell survival (based on ubiquitin promoter-driven *Luc* expression) and osteogenic differentiation (based on osteocalcin promoter-driven *Luc* expression). The rats were anesthetized by continuous administration of 1.0−3.0% isoflurane mixed with 100% medical-grade oxygen. A percutaneous injection of luciferin was administered locally (2.5 mg/injection) into the site of the defect 5 min before imaging commenced. Light emission was evaluated using the Xenogen IVIS Spectrum system (Caliper Life Sciences, Hopkinton, MA). The exposure time was set automatically, and bioluminescence was quantified as the total signal normalized to the length of the exposure and the area of the region of interest.

Bone Regeneration Analysis Using Micro Computed Tomography. In vivo bone formation at sites of regeneration was evaluated over time by performing microCT analyses. To quantify bone regeneration and compare it among several samples, a standard method must be used. The microCT procedures used for this study were described in detail by Kallai et al.[43]

In vivo microCT scanning of the anesthetized rats was performed on day 1 and at weeks 2, 4, 6, and 12 postoperatively by using a preclinical cone-beam in vivo microCT system (vivaCT 40; Scanco Medical AG, Brüttisellen, Switzerland). Microtomographic slices were acquired using an X-ray tube potential of 55 kVp, after which they were reconstructed at a voxel size of 21 μm. After locating the defect region, the defect margins were aligned to a standard position and a cylindrical volume of interest (VOI; 1.68 mm in diameter, 2.52 mm in height) was defined for a 3D histomorphometric evaluation. A constrained 3D Gaussian filter (σ = 0.8 and support = 1) was used to partly suppress the noise in the volumes. The bone tissue was segmented from marrow and soft tissue by using a global thresholding procedure.[44] In addition to visual assessments of the structural images, morphometric indices were determined on the basis of microtomographic data sets by using direct 3D morphometry.[45]

Evaluation of regenerated bone tissue was made by a qualitative assessment of bone structure based on 2D cross sections and 3D images, and a quantitative assessment of bone structure based on microtomographic data sets created using direct 3D morphometry. The following morphometric indices were determined for newly formed bone in the regeneration sites: (1) volume of mineralized bone tissue [BV, mm^3]; (2) percentage of bone regeneration, calculated as the ratio between added BV (BV − BV_{day1}) and the average BV of native vertebrae (n = 5) in a similar cylindrical VOI (bone regeneration, %); (3) connectivity density [Conn.Dens, $1/mm^3$], which was derived from the Euler number,[46] a topologic measure used to describe the porosity of the bone sample and to show the extent of branching in the bone structure; (4) average bone thickness [B.Th, mm], calculated as the average thickness of all bone voxels and abbreviated as "Tb. Th*" by Hildebrand et al., 1999; and (5) bone mineral density (BMD, mg of hydroxyapatite [HA]/cm^3], derived from comparison of X-ray attenuation in the scanned bone sample with that of hydroxyapatite standards.

Histological and Immunohistochemical Analyses. The harvested rat-tail vertebrae were cleaned from intact muscles and soft tissue and were fixed in 4% formalin for 48 h. They were then decalcified by soaking in a 0.5 M EDTA solution (pH 7.4) for 14 days, passed through an increasing-grade series of ethanol baths, and embedded in paraffin. Five-micrometer-thick sections were cut from each paraffin block with the aid of a motorized microtome (Leica Microsystems, Nussloch, Germany). The slides were heated at 65 °C for 45 min; this process was followed

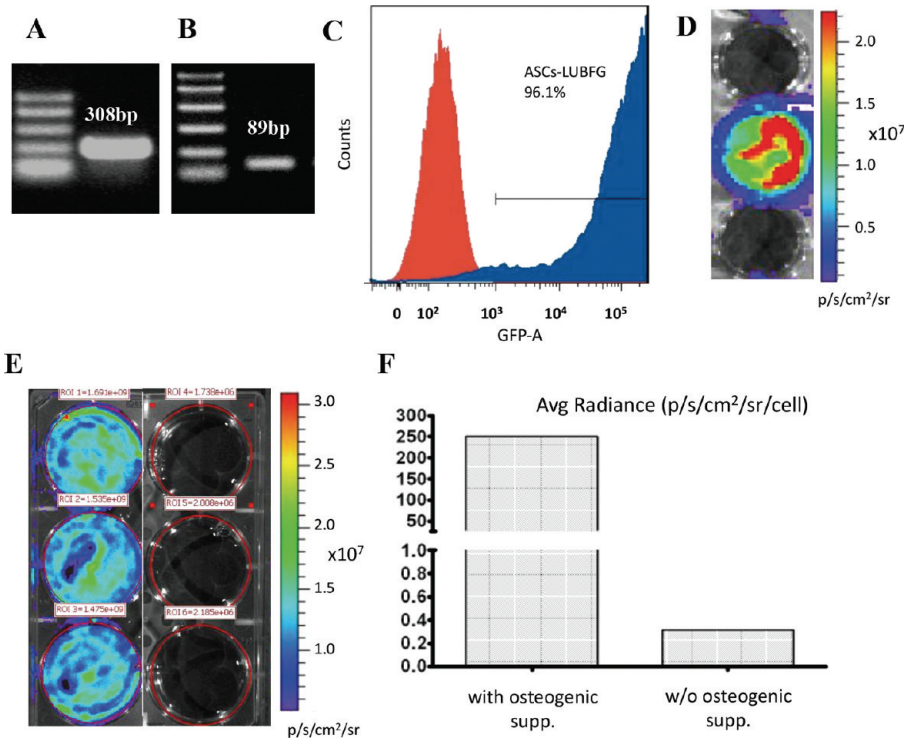

Figure 1. Stem cell labeling with reporter genes. Porcine ASCs were transduced with either the lentiviral vector LUBFG (A, C, D) or Oc-Luc2 (B, E, F). DNA extracted from the transduced cells was tested for Luc (A) and osteocalcin promoter (B) presence using PCR. *GFP* expression by LUBFG-transduced cells was evaluated using FACS (C) and *Luc* expression was verified using BLI (D). The *Oc-Luc2* reporter gene activity in the Oc-Luc2-transduced ASCs was verified after the cells had had 14 days of osteogenic differentiation in the presence of osteogenic supplements. The cells were imaged in vitro (E), and the signal was quantified and compared with signals of cells transduced with the vector but grown without osteogenic supplements (F). ROI = region of interest.

by deparaffinization. Hematoxylin and eosin (H&E) staining and bone matrix-specific Masson's trichrome staining were performed as previously reported.[25,31]

An immunohistochemical assay was performed to detect the expression of porcine vimentin on paraffin sections of fused spines by using a HISTOMOUSE-SP kit (Catalog No. 95-9541, Zymed Laboratories, South San Francisco, CA, USA). Sections of tissue were deparaffinized with xylene, rehydrated in a descending-grade series of ethanol baths, and rinsed in PBS. The antigens were retrieved enzymatically by using an antigen retrieval kit (Catalog No. ab8212, Abcam, Cambridge Science Park, Cambridge, U.K.). Endogenous peroxidase activity was removed by treatment with 0.1% H_2O_2 for 10 min. A primary antibody that reacts with human, porcine, and equine vimentin, but not with mouse vimentin (Catalog No. ab8069, Abcam Ltd., Cambridge Science Park, Cambridge, U.K.), was diluted 1:10 in PBS and applied to the slides for 1 h at room temperature. After incubation with the primary antibody, the slides were rinsed in PBS and a secondary goat anti-mouse IgG antibody (biotin-conjugated; Zymed, San Francisco, CA, USA) was applied to the slides at room temperature for 10 min. After they had been washed with PBS, the slides were incubated with horseradish peroxidase conjugated to streptavidin and then stained with 3-amino-9-ethylcarbazole dye. The slides were counterstained with hematoxylin, washed, attached using GVA mounting solution (Zymed, San Francisco, CA, USA), and visualized with the aid of light microscopy.

Statistical Analysis. All mean values in Results and in the figures are displayed with their standard errors. Comparisons between the ASC-BMP6 and control groups at each time point for bone regeneration percentage, Conn.Dens, B.Th, and BMD were performed using the Student *t* test. Linear mixed-effects models were used for longitudinal analyses of *Luc* reporter gene expression, bone regeneration rate, Conn.Dens, BMD, and B.Th across time. *Luc* expression was log-transformed to ensure normality in the longitudinal analysis. Whenever multiple comparisons were involved, the significance level of each individual test was adjusted using the Bonferroni correction. The increasing percentages of bone regeneration at weeks 2, 4, and 6 were calculated using linear regression. Analyses were performed using SAS software, version 9.2 (SAS Institute Inc., Cary, NC).

RESULTS

Stem Cell Labeling with Reporter Genes. Porcine ASCs were isolated from fresh adipose tissue, expanded in culture, and infected with a lentiviral vector (LUBFG or Oc-Luc2). Their successful infection was verified by PCRs of genomic DNA extracted from pASC-LUBFG cells (Figure 1A) and pASC-Oc-Luc2 cells (Figure 1B), which showed that both cell types harbored the appropriate transgene as expected. The percentage of *GFP*-expressing pASC-LUBFG cells was evaluated using flow cytometry, which showed that more than 96% of the cells were infected with LUBFG (Figure 1C). Furthermore, *Luc* expression by the pASC-LUBFG cells was evident using in vitro BLI (Figure 1D). To verify successful infection with the Lenti-Oc-Luc2 vector, the infected cells were grown with and without osteogenic supplements in vitro and imaged on day 14 after osteogenesis induction using BLI. The results showed that the

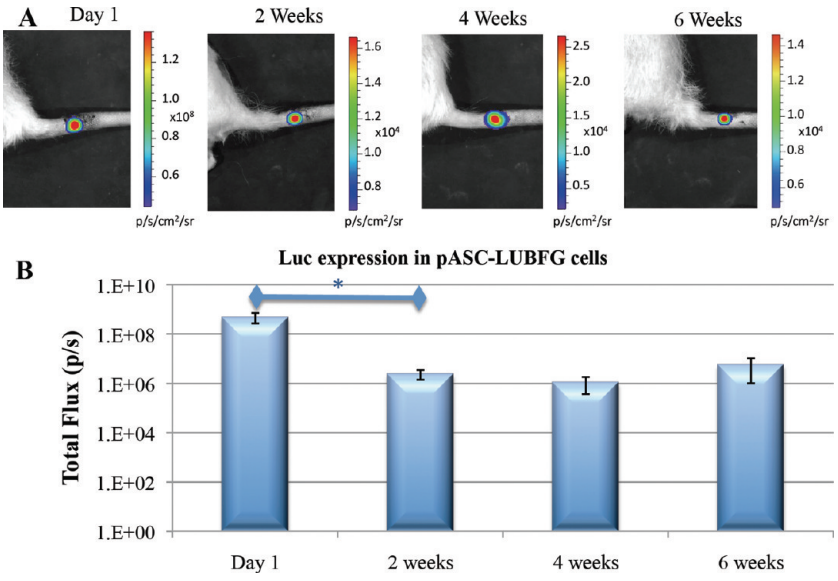

Figure 2. Stem cell survival in vivo: bioluminescence imaging. pASC-LUBFG cells were injected into vertebral bone voids. At designated time points, luciferin substrate was injected subcutaneously into the operated sites of rat tails. This was followed by BLI (A) and quantitative analysis (B). $n = 7$; bars represent ±SE; $^*p < 0.05$.

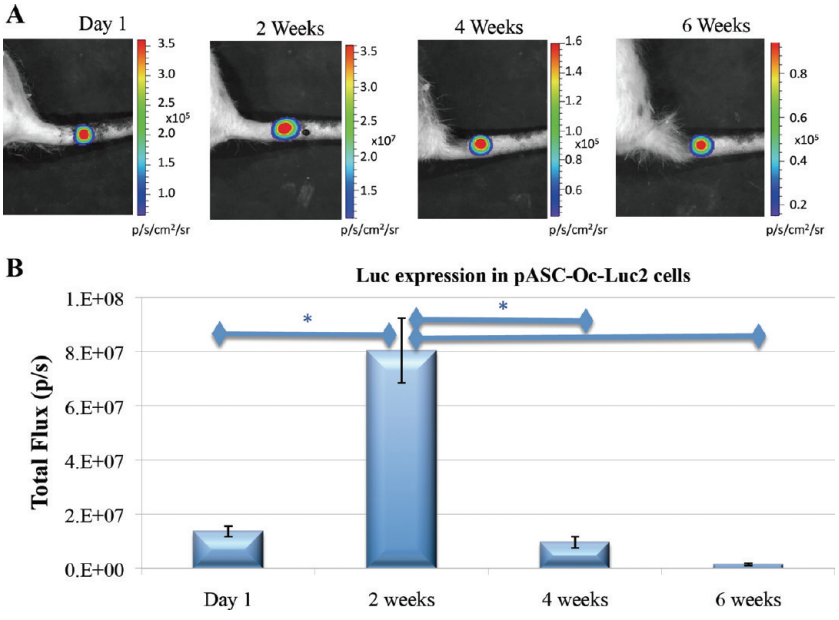

Figure 3. Osteogenic differentiation of engineered ASCs monitored by bioluminescence. pASC-Oc-Luc2 cells were injected into vertebral bone voids. At several time points, luciferin substrate was injected subcutaneously into the operated sites of rat tails. This was followed by BLI (A) and quantitative analysis (B). $n = 6$; bars represent ±SE; $^*p < 0.05$.

Luc2 reporter gene was expressed only in osteogenically differentiated pASC-Oc-Luc2 cells (Figure 1E,F).

Optical Imaging of Donor Cell Survival and Osteogenic Differentiation in Vivo. ASCs were infected with two reporter genes so that we could monitor cell survival (constitutively expressed luciferase) and osteogenic differentiation (luciferase driven by osteocalcin promoter). In vivo BLI demonstrated a highly localized signal from the site of implantation (Figure 2A). The quantitative analysis of *Luc* expression by cells engineered using the LUBFG construct showed that there was a rapid loss of viable cells in the site of implantation during the first 2 weeks (Figure 2B). However, after 2 weeks, no further significant change in reporter gene expression was observed. The results indicate that *Luc* expression changes significantly over time ($p = 0.0003$). Pairwise comparisons among the four time points suggest that *Luc* expression is significantly higher on day 1 than at weeks 2, 4, and 6. *Luc* expression appeared to remain stable throughout weeks 2, 4, and 6; no significant differences in *Luc* expression were identified among these time points.

A completely different pattern was revealed when we examined cells infected with the *Oc-Luc* construct (Figure 3A,B). At the first imaging session—24 h postimplantation and 48 h

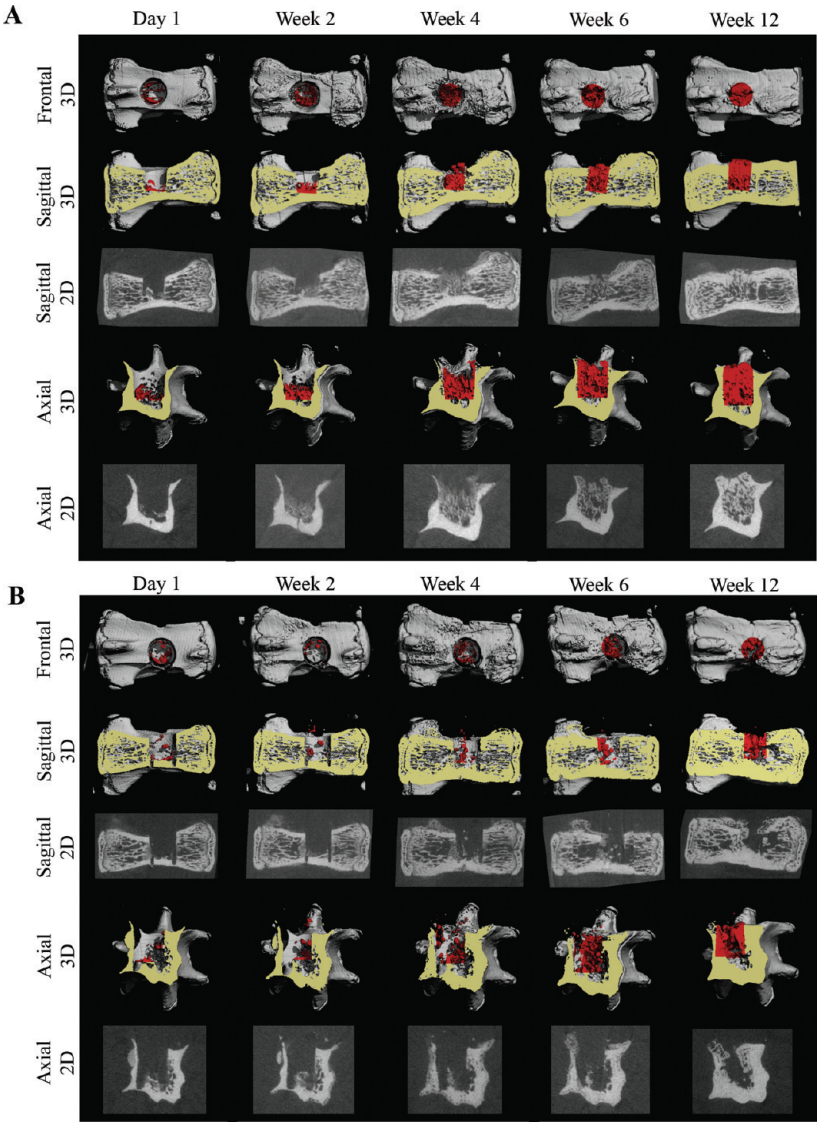

Figure 4. Imaging of ASC-based vertebral bone void repair. Longitudinal microCT-based imaging of ASC-BMP6 (A) and FG-only control (B) cells, 1 day and 2, 4, 6, and 12 weeks after surgery. Sagittal and axial cross sections of vertebrae are shown in 3D and 2D images. A quantitative analysis of bone formation in the cylindrical (1.68 mm in diameter, 2.52 mm in height) VOI (highlighted in red) was performed (shown in Figure 5).

postnucleofection—relatively low expression levels of *Luc* were detected, whereas significantly higher levels of gene expression were found 2 weeks after implantation. At the week 4 and week 6 observations, it was clear that gene expression had rapidly declined compared with the previous observation (Figure 3B). The results indicate that osteocalcin promoter-driven *Luc* expression changes significantly over time ($p = 0.0262$). Pairwise comparisons of *Luc* expression at the four time points suggest that *Luc* expression reaches its peak at week 2 (when the expression level is significantly higher than that at day 1 and weeks 4 and 6). No significant differences in *Luc* expression were identified when we compared observations on day 1 and at weeks 4 and 6. This expression profile follows a previously reported expression profile of osteocalcin, a marker for bone formation,[47] during osteogenesis in vivo.[48,49]

Qualitative and Quantitative MicroCT-Based Analyses of Vertebral Bone Regeneration. MicroCT imaging of defects, performed 24 h after surgery, showed that the void volumes (VOI − BV_{day1}) of all samples were very similar (SE ± 1.3% of the void volume). Over time, prominent new bone tissue formation was detected in the vertebral bone void sites. Compared with defects in the FG-only control group, accelerated bone formation was evident in defects in the ASC-BMP6 group (Figures 4 and 5). The 2D tomographic images show regenerative changes in the morphological characteristics of bone over time (Figure 4). The morphological characteristics of regenerated bone in the ASC-BMP6 group became more similar to those of native vertebrae, with trabecular bone in the interior and a thick cortex (Figure 4A, at 6 and 12 weeks). A quantitative analysis of newly formed bone in the cylindrical VOI showed that bone regeneration in the ASC-BMP6 group was significantly higher than bone regeneration in the FG-only control group over time. The main bone growth and mineralization in the site of the defect occurred between weeks 2 and 6 postsurgery in both groups. However, the rate of regeneration during this period was also approximately two times higher in the ASC-BMP6 group than in the FG-only control group, based on the slope of the

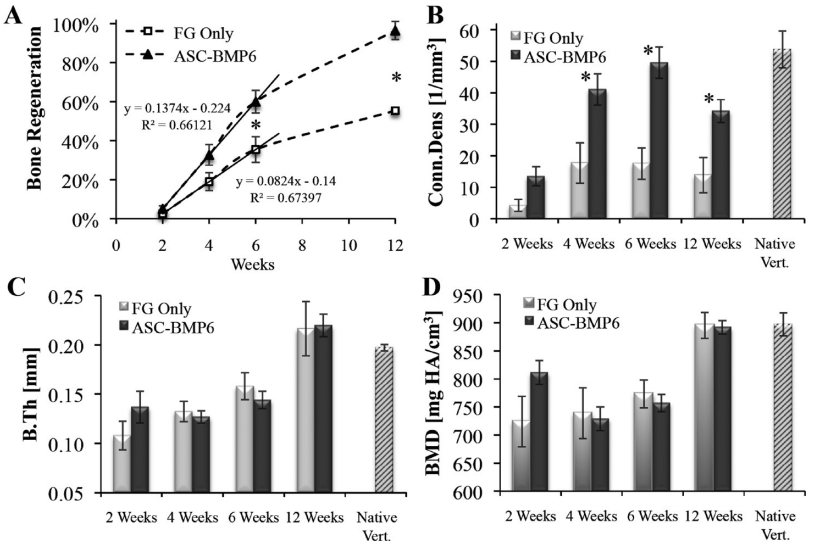

Figure 5. Quantitative analysis of ASC-based vertebral bone void repair. Longitudinal microCT-based quantitative analysis of bone formation in the cylindrical VOI. n = 13 (ASC-BMP6); n = 5 (FG-only control, at week 12 n = 3); n = 5 (native vert.); Bars represent ± SE. Statistically significant differences (two-tailed homoscedastic Student t tests) between the ASC-BMP6 and FG-only control groups are marked, *$p < 0.05$.

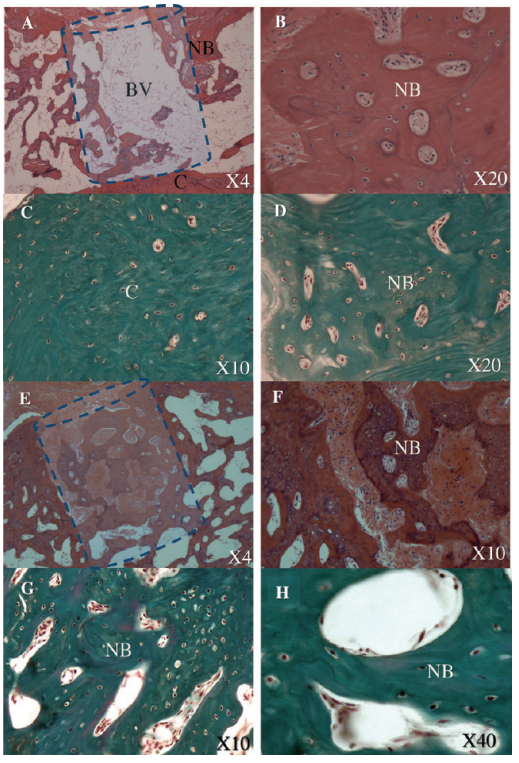

Figure 6. Stem cell and gene-based bone void repair: histological analysis. At week 12 the rats were euthanized and their tails harvested. The histological analysis was performed using standard H&E (A, B, E, F) and bone matrix-specific Masson's trichrome (C, D, G, H) staining. The defect treated with FG alone is shown in panels A—D, whereas the defect repaired with gene-modified stem cells is shown in panels E—H. The dashed line shows the estimated borders of the defect. BV: bone void. NB: new bone formation. C: vertebral cortex.

linear trend line (0.1374 vs 0.0824) demonstrated in Figure 5A. The difference in rates (or slopes) between the two groups is significant (p = 0.0378).

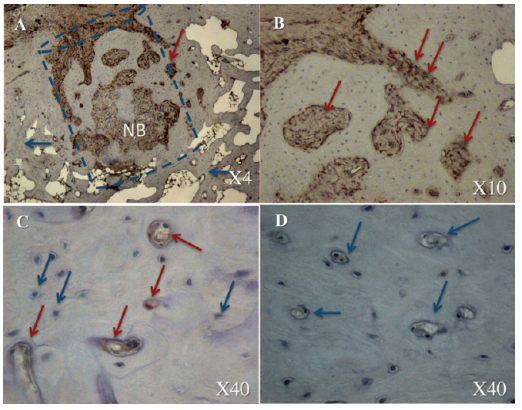

Figure 7. Stem cell contribution to the bone void repair: immunohistochemical analysis. The dashed line shows the estimated borders of the defect. NB: new bone formation. The blue arrows indicate a native host cell, and the red arrows indicate donor porcine cells. The defect repaired with gene-modified stem cells is shown in panels A—C, whereas defect treated with FG alone is shown in panel D.

Significantly higher values of Conn.Dens (Figure 5B) were found at weeks 4, 6, and 12 postsurgery, indicating that the microstructure of regenerated bone in the ASC-BMP6 group is more branched and thus may be more biomechanically competent than nontreated regenerated bone. No significant differences between groups were found in the thickness and mineral density of regenerated bone (Figure 5C,D).

Morphological Analysis of Bone Repair and the Donor Cell Contribution to New Tissue Formation. The histological analysis confirmed our imaging-based findings and demonstrated remarkable bone formation and defect regeneration in bone voids in which the engineered stem cells had been implanted. Standard H&E (Figure 6A,B,E,F) and bone matrix-specific Masson's trichrome staining (Figure 6C,D,G,H) revealed well-organized trabecular and cortex bone at the site of the defect. Light microscopy of the bone architecture revealed an organized bone mass with a lamellar microstructure containing compartments of

bone marrow that highly resembled intact vertebral bone tissue morphologically (Figure 6E−H). Conversely, minor bone formation was found in the control group treated with FG alone, which was injected in the same manner (Figure 6A−D). No remnants of FG were found in either group. The IHC analysis of the sections using an antibody against porcine vimentin revealed the new bone tissue formed partially constituted of donor porcine ASCs (Figure 7). Thus we can conclude that the pASCs were differentiated into bone progenitor cells and actively contributed to the bone regeneration process.

DISCUSSION

Although vertebral fractures constitute a major problem for both elderly and military populations, a biological solution for such injuries has not yet been found. Osteoporotic patients cannot be treated with conventional spine implants because of their low bone mass. Furthermore, current methods of vertebroplasty do not induce bone formation. Injured soldiers are presently removed from active duty for long periods of time until their vertebrae are healed. In this study we have demonstrated an injectable stem cell therapy that has a potential to accelerate vertebral bone repair. This therapeutic approach might be relevant for both patient populations.

A vertebral bone void model was recently reported in rodents.[14] In the study by Liang et al., two different-sized defects ($2 \times 3 \times 1.5$ mm and $2 \times 3 \times 3$ mm) were created using globular burrs. Neither defect was completely repaired after 8 weeks; however, natural bone regeneration was observed in both.[14] In the present study we developed a single, reproducible defect to see if we could accelerate the natural regenerative process by using gene-modified ASCs. Because only one defect was created in each animal, we were able to assess the regenerative process in each defect independently from that in other defects. The defects were created in a well-controlled environment, and their proximity to the surface enabled longitudinal cell tracking in vivo.

Our results indicate a rapid loss of viable cells at the site of implantation during the first 2 weeks postinjection (Figure 3B). We speculate that the cause of this decrease in viable cell survival is 2-fold: (1) lack of vascularization and consequent lack of nutrients at the site of the defect; and (2) apoptosis, a natural accompaniment to the osteogenic differentiation process. There has also been a great deal of debate concerning whether MSCs actually differentiate in vivo or merely serve as paracrine inducers. In this study gene-modified stem cells not only survived in the implantation site for 12 weeks but also differentiated and contributed to full regeneration of bone tissue in the vertebral body.

The regenerative potential of bone tissue declines with age, thus additional regenerative agents such as MSCs are required for successful bone repair. Using our model the native regenerative ability of bone tissue was not compromised in this study, and thus some tissue formation was evident in the control group, which was treated with FG alone. However, due to the relatively large volume of bone void created, defects in the control group were not fully regenerated (Figure 4B). Conversely, use of genetically modified stem cells not only increased the extent of bone formation and the eventual volume of bone tissue inside the defect (Figure 4A) but also significantly accelerated the repair process (Figure 5A). The morphometric indices, average bone thickness, and mineral density of regenerated bone were similar in both groups. The values of these indices increased from week 6 to week 12, to a level similar to values of native vertebrae (Figure 5C,D), indicating that a 12 week period is sufficient for monitoring the healing process.

Stem cell tracking is critical to document the development of every cell-mediated therapy. In this study we aimed to investigate whether we could track donor cells inside the defect area and estimate their contribution to the regenerative process. We were able to show that the donor ASCs not only served as in vivo "bioreactors" for rhBMP6 secretion to initiate the bone formation process but also actively participated in the tissue regeneration itself. In a previous study we showed that ASC-BMP6 cells contribute to bone formation in vivo;[31] here we were able to show that the labeled and nucleofected cells differentiate into bone-forming cells and express the osteogenic marker gene *osteocalcin*. The osteocalcin promoter-driven *Luc2* expression significantly increased 2 weeks after transplantation, suggesting that cells that survive the first few weeks undergo osteogenic differentiation and contribute to bone tissue formation.

We find it very encouraging that new bone that formed in bone voids treated by gene-modified cells did not differ biologically or structurally from bone that formed in the voids of control animals treated with FG alone (Figure 5C,D). We conclude from this that the development of genetically engineered bone tissue resembles that of natural bone tissue created via the natural regeneration process, although in a more accelerated manner and eventually reaching larger volumes. We previously showed that the nonviral, transient overexpression of BMP results in the secretion of rhBMP6 at physiological levels,[31] and thus bone formation occurs in a natural and safe manner in a controlled environment compared with bone formation in the setting of conventional rhBMP protein therapy.

The proposed therapy, which involves the use of genetically modified adipose tissue-derived adult stem cells, has great potential for various applications of bone tissue regeneration and spine therapy. In the present study we identified engineered bone tissue that morphologically and structurally resembled that of native tissue. Encouraged by the results of this study, we intend to develop this model in large animals in order to promote the translation of this research into clinical practice. However, it is important to note that VCFs are a complication of osteoporosis and, as such, treating such fractures will be efficient only if the underlying disease is treated as well. We envision that gene-modified cell therapy could be combined with an appropriate treatment for osteoporosis, thus leading to a substantial improvement in the quality of life of these patients.

AUTHOR INFORMATION

Corresponding Author

*Stem Cell Therapeutics Research Laboratory, Regenerative Medicine Institute, Department of Surgery, Cedars-Sinai Medical Center, 8700 Beverly Blvd., SSB, 3rd Floor, Rm 329, Los Angeles, CA 90048. E-mail: dgaz@cc.huji.ac.il. Phone: 310-423-8070.

Author Contributions

‡These authors equally contributed to this manuscript.

ACKNOWLEDGMENT

We acknowledge funding from the Telemedicine and Advanced Technology Research Center (TATRC), the U.S. Army Medical Research and Materiel Command (Grant No. 0821700), the National Institutes of Health (Grant No. R01AR056694) and the California Institute for Regenerative Medicine (CIRM

RT2-02057). We also acknowledge funding from the Ministry of Science and Technology, State of Israel, which supports a "Levi Eshkol fellowship" to I.K. We thank Dr. Joseph C. Wu from Stanford University for the LUBFG construct and Dr. Eduardo Marbán from Cedars-Sinai Medical Center for the lentiviral vector.

REFERENCES

(1) Ray, N. F.; Chan, J. K.; Thamer, M.; Melton, L. J., 3rd. Medical expenditures for the treatment of osteoporotic fractures in the United States in 1995: report from the National Osteoporosis Foundation. *J. Bone Miner. Res.* **1997**, *12* (1), 24–35.

(2) Kanis, J. Assessment of osteoporosis at the primary health-care level. *World Health Organization Collaborating Centre for Metabolic Bone Diseases*; University of Sheffield: Sheffield, U.K., 2007.

(3) Borgstrom, F.; Zethraeus, N.; Johnell, O.; Lidgren, L.; Ponzer, S.; Svensson, O.; Abdon, P.; Ornstein, E.; Lunsjo, K.; Thorngren, K. G.; Sernbo, I.; Rehnberg, C.; Jonsson, B. Costs and quality of life associated with osteoporosis-related fractures in Sweden. *Osteoporosis Int.* **2006**, *17* (5), 637–50.

(4) Silverman, S. L.; Minshall, M. E.; Shen, W.; Harper, K. D.; Xie, S. Health-Related Quality of Life Subgroup of the Multiple Outcomes of Raloxifene Evaluation, S. The relationship of health-related quality of life to prevalent and incident vertebral fractures in postmenopausal women with osteoporosis: results from the Multiple Outcomes of Raloxifene Evaluation Study. *Arthritis Rheum.* **2001**, *44* (11), 2611–9.

(5) Johnell, O.; Kanis, J. A. An estimate of the worldwide prevalence and disability associated with osteoporotic fractures. *Osteoporosis Int.* **2006**, *17* (12), 1726–33.

(6) Truumees, E.; Hilibrand, A.; Vaccaro, A. R. Percutaneous vertebral augmentation. *Spine J.* **2004**, *4* (2), 218–29.

(7) Helgeson, M.; Lehman, R.; Sieg, R.; Cooper, P.; Rosner, M.; Bellabarba, C. Low lumbar burst fractures: A unique fracture mechanism sustained in our current overseas conflicts. *Spine J.* **2008**, *8*, 136S.

(8) Islinger, R. B.; Kuklo, T. R.; Polly, D. W., Jr. Spine fractures in active duty soldiers and their return to duty rate. *Mil. Med.* **1998**, *163* (8), 536–9.

(9) Kornberg, M.; Rechtine, G. R.; Herndon, W. A.; Reinert, C. M.; Dupuy, T. E. Surgical stabilization of thoracic and lumbar spine fractures: a retrospective study in a military population. *J. Trauma* **1984**, *24* (2), 140–6.

(10) Belmont, P. J., Jr.; Taylor, K. F.; Mason, K. T.; Shawen, S. B.; Polly, D. W., Jr.; Klemme, W. R. Incidence, epidemiology, and occupational outcomes of thoracolumbar fractures among U.S. Army aviators. *J. Trauma* **2001**, *50* (5), 855–61.

(11) Black, D. M.; Cummings, S. R.; Karpf, D. B.; Cauley, J. A.; Thompson, D. E.; Nevitt, M. C.; Bauer, D. C.; Genant, H. K.; Haskell, W. L.; Marcus, R.; Ott, S. M.; Torner, J. C.; Quandt, S. A.; Reiss, T. F.; Ensrud, K. E. Randomised trial of effect of alendronate on risk of fracture in women with existing vertebral fractures. Fracture Intervention Trial Research Group. *Lancet* **1996**, *348* (9041), 1535–41.

(12) Greenspan, S. L.; Bone, H. G.; Ettinger, M. P.; Hanley, D. A.; Lindsay, R; Zanchetta, J. R.; Blosch, C. M.; Mathisen, A. L.; Morris, S. A.; Marriott, T. B.; Group., T. o. O. w. P. H. S. Effect of recombinant human parathyroid hormone (1−84) on vertebral fracture and bone mineral density in postmenopausal women with osteoporosis: a randomized trial. *Ann. Intern. Med.* **2007**, *146* (5), 326–39.

(13) Parfitt, A. M. Implications of architecture for the pathogenesis and prevention of vertebral fracture. *Bone* **1992**, *13* (Suppl. 2), S41–7.

(14) Liang, H.; Wang, K.; Shimer, A. L.; Li, X.; Balian, G.; Shen, F. H. Use of a bioactive scaffold for the repair of bone defects in a novel reproducible vertebral body defect model. *Bone* **2010**, *47* (2), 197–204.

(15) Furtado, N.; Oakland, R. J.; Wilcox, R. K.; Hall, R. M. A biomechanical investigation of vertebroplasty in osteoporotic compression fractures and in prophylactic vertebral reinforcement. *Spine* **2007**, *32* (17), E480–7.

(16) Buchbinder, R.; Osborne, R. H.; Ebeling, P. R.; Wark, J. D.; Mitchell, P.; Wriedt, C.; Graves, S.; Staples, M. P.; Murphy, B. A randomized trial of vertebroplasty for painful osteoporotic vertebral fractures. *N. Engl. J. Med.* **2009**, *361* (6), 557–68.

(17) Kallmes, D. F.; Comstock, B. A.; Heagerty, P. J.; Turner, J. A.; Wilson, D. J.; Diamond, T. H.; Edwards, R.; Gray, L. A.; Stout, L.; Owen, S.; Hollingworth, W.; Ghdoke, B.; Annesley-Williams, D. J.; Ralston, S. H.; Jarvik, J. G. A Randomized Trial of Vertebroplasty for Osteoporotic Spinal Fractures. *N. Engl. J. Med.* **2009**, *361* (6), 569–79.

(18) Kobayashi, H.; Turner, A. S.; Seim, H. B., 3rd; Kawamoto, T.; Bauer, T. W. Evaluation of a silica-containing bone graft substitute in a vertebral defect model. *J. Biomed. Mater. Res., Part A* **2010**, *92* (2), 596–603.

(19) Phillips, F. M.; Turner, A. S.; Seim, H. B., 3rd; MacLeay, J.; Toth, C. A.; Pierce, A. R.; Wheeler, D. L. In vivo BMP-7 (OP-1) enhancement of osteoporotic vertebral bodies in an ovine model. *Spine J.* **2006**, *6* (5), 500–6.

(20) Bruder, S. P.; Fink, D. J.; Caplan, A. I. Mesenchymal stem cells in bone development, bone repair, and skeletal regeneration therapy. *J. Cell. Biochem.* **1994**, *56* (3), 283–94.

(21) Caplan, A. I. Mesenchymal stem cells. *J. Orthop. Res.* **1991**, *9* (5), 641–50.

(22) Dennis, J. E.; Merriam, A.; Awadallah, A.; Yoo, J. U.; Johnstone, B.; Caplan, A. I. A quadripotential mesenchymal progenitor cell isolated from the marrow of an adult mouse. *J. Bone Miner. Res.* **1999**, *14* (5), 700–9.

(23) Gazit, D.; Turgeman, G.; Kelley, P.; Wang, E.; Jalenak, M.; Zilberman, Y.; Moutsatsos, I. Engineered pluripotent mesenchymal cells integrate and differentiate in regenerating bone: a novel cell-mediated gene therapy. *J. Gene Med.* **1999**, *1* (2), 121–33.

(24) Wang, J. C.; Kanim, L. E.; Yoo, S.; Campbell, P. A.; Berk, A. J.; Lieberman, J. R. Effect of regional gene therapy with bone morphogenetic protein-2-producing bone marrow cells on spinal fusion in rats. *J. Bone Joint Surg. Am.* **2003**, *85-A* (5), 905–11.

(25) Turgeman, G.; Pittman, D. D.; Muller, R.; Kurkalli, B. G.; Zhou, S.; Pelled, G.; Peyser, A.; Zilberman, Y.; Moutsatsos, I. K.; Gazit, D. Engineered human mesenchymal stem cells: a novel platform for skeletal cell mediated gene therapy. *J. Gene Med.* **2001**, *3* (3), 240–51.

(26) Moutsatsos, I. K.; Turgeman, G.; Zhou, S.; Kurkalli, B. G.; Pelled, G.; Tzur, L.; Kelley, P.; Stumm, N.; Mi, S.; Muller, R.; Zilberman, Y.; Gazit, D. Exogenously regulated stem cell-mediated gene therapy for bone regeneration. *Mol. Ther.* **2001**, *3* (4), 449–61.

(27) Hasharoni, A.; Zilberman, Y.; Turgeman, G.; Helm, G. A.; Liebergall, M.; Gazit, D. Murine spinal fusion induced by engineered mesenchymal stem cells that conditionally express bone morphogenetic protein-2. *J. Neurosurg. Spine* **2005**, *3* (1), 47–52.

(28) Kimelman-Bleich, N.; Pelled, G.; Sheyn, D.; Kallai, I.; Zilberman, Y.; Mizrahi, O.; Tal, Y.; Tawackoli, W.; Gazit, Z.; Gazit, D. The use of a synthetic oxygen carrier-enriched hydrogel to enhance mesenchymal stem cell-based bone formation in vivo. *Biomaterials* **2009**, *30* (27), 4639–48.

(29) Gafni, Y.; Pelled, G.; Zilberman, Y.; Turgeman, G.; Apparailly, F.; Yotvat, H.; Galun, E.; Gazit, Z.; Jorgensen, C.; Gazit, D. Gene therapy platform for bone regeneration using an exogenously regulated, AAV-2-based gene expression system. *Mol. Ther.* **2004**, *9* (4), 587–95.

(30) Lin, Y.; Tang, W.; Wu, L.; Jing, W.; Li, X.; Wu, Y.; Liu, L.; Long, J.; Tian, W. Bone regeneration by BMP-2 enhanced adipose stem cells loading on alginate gel. *Histochem. Cell Biol.* **2008**, *129* (2), 203–10.

(31) Sheyn, D.; Pelled, G.; Zilberman, Y.; Talasazan, F.; Frank, J. M.; Gazit, D.; Gazit, Z. Nonvirally engineered porcine adipose tissue-derived stem cells: use in posterior spinal fusion. *Stem Cells* **2008**, *26* (4), 1056–64.

(32) Sheyn, D.; Ruthemann, M.; Mizrahi, O.; Kallai, I.; Zilberman, Y.; Tawackoli, W.; Kanim, L. E.; Zhao, L.; Bae, H.; Pelled, G.; Snedeker, J. G.; Gazit, D. Genetically modified mesenchymal stem cells induce mechanically stable posterior spine fusion. *Tissue Eng., Part A* **2010**, *16* (12), 3679–86.

(33) Aslan, H.; Sheyn, D.; Gazit, D. Genetically engineered mesenchymal stem cells: applications in spine therapy. *Regen. Med.* **2009**, *4* (1), 99–108.

(34) Dubois, S. G.; Floyd, E. Z.; Zvonic, S.; Kilroy, G.; Wu, X.; Carling, S.; Halvorsen, Y. D.; Ravussin, E.; Gimble, J. M. Isolation of human adipose-derived stem cells from biopsies and liposuction specimens. *Methods Mol. Biol.* **2008**, *449*, 69–79.

(35) Li, Z.; Suzuki, Y.; Huang, M.; Cao, F.; Xie, X.; Connolly, A. J.; Yang, P. C.; Wu, J. C. Comparison of reporter gene and iron particle labeling for tracking fate of human embryonic stem cells and differentiated endothelial cells in living subjects. *Stem Cells* **2008**, *26* (4), 864–73.

(36) Sun, N.; Lee, A.; Wu, J. C. Long term non-invasive imaging of embryonic stem cells using reporter genes. *Nat. Protoc.* **2009**, *4* (8), 1192–201.

(37) Morrison, N. A.; Shine, J.; Fragonas, J. C.; Verkest, V.; McMenemy, M. L.; Eisman, J. A. 1,25-dihydroxyvitamin D-responsive element and glucocorticoid repression in the osteocalcin gene. *Science* **1989**, *246* (4934), 1158–61.

(38) Dull, T.; Zufferey, R.; Kelly, M.; Mandel, R. J.; Nguyen, M.; Trono, D.; Naldini, L. A third-generation lentivirus vector with a conditional packaging system. *J. Virol.* **1998**, *72* (11), 8463–71.

(39) Celeste, A. J.; Rosen, V.; Buecker, J. L.; Kriz, R.; Wang, E. A.; Wozney, J. M. Isolation of the human gene for bone gla protein utilizing mouse and rat cDNA clones. *EMBO J.* **1986**, *5* (8), 1885–90.

(40) Aslan, H.; Zilberman, Y.; Kandel, L.; Liebergall, M.; Oskouian, R. J.; Gazit, D.; Gazit, Z. Osteogenic differentiation of noncultured immunoisolated bone marrow-derived CD105+ cells. *Stem Cells* **2006**, *24* (7), 1728–37.

(41) Steinhardt, Y.; Aslan, H.; Regev, E.; Zilberman, Y.; Kallai, I.; Gazit, D.; Gazit, Z. Maxillofacial-derived stem cells regenerate critical mandibular bone defect. *Tissue Eng., Part A* **2008**, *14* (11), 1763–73.

(42) Sheyn, D.; Pelled, G.; Netanely, D.; Domany, E.; Gazit, D. The effect of simulated microgravity on human mesenchymal stem cells cultured in an osteogenic differentiation system: a bioinformatics study. *Tissue Eng., Part A* **2010**, *16* (11), 3403–12.

(43) Kallai, I.; Mizrahi, O.; Tawackoli, W.; Gazit, Z.; Pelled, G.; Gazit, D. Microcomputed tomography-based structural analysis of various bone tissue regeneration models. *Nat. Protoc.* **2011**, *6* (1), 105–10.

(44) Müller, R.; Ruegsegger, P. Micro-tomographic imaging for the nondestructive evaluation of trabecular bone architecture. *Stud. Health Technol. Inform.* **1997**, *40*, 61–79.

(45) Hildebrand, T.; Laib, A.; Müller, R.; Dequeker, J.; Ruegsegger, P. Direct three-dimensional morphometric analysis of human cancellous bone: microstructural data from spine, femur, iliac crest, and calcaneus. *J. Bone Miner. Res.* **1999**, *14* (7), 1167–74.

(46) Odgaard, A.; Gundersen, H. J. Quantification of connectivity in cancellous bone, with special emphasis on 3-D reconstructions. *Bone* **1993**, *14* (2), 173–82.

(47) Boivin, G.; Morel, G.; Lian, J. B.; Anthoine-Terrier, C.; Dubois, P. M.; Meunier, P. J. Localization of endogenous osteocalcin in neonatal rat bone and its absence in articular cartilage: effect of warfarin treatment. *Virchows Arch. A: Pathol. Anat. Histopathol.* **1990**, *417* (6), 505–12.

(48) Sheyn, D.; Kimelman-Bleich, N.; Pelled, G.; Zilberman, Y.; Gazit, D.; Gazit, Z. Ultrasound-based nonviral gene delivery induces bone formation in vivo. *Gene Ther.* **2008**, *15* (4), 257–66.

(49) Iris, B.; Zilberman, Y.; Zeira, E.; Galun, E.; Honigman, A.; Turgeman, G.; Clemens, T.; Gazit, Z.; Gazit, D. Molecular imaging of the skeleton: quantitative real-time bioluminescence monitoring gene expression in bone repair and development. *J, Bone Miner. Res.* **2003**, *18* (3), 570–8.